



## 24 **Abstract**

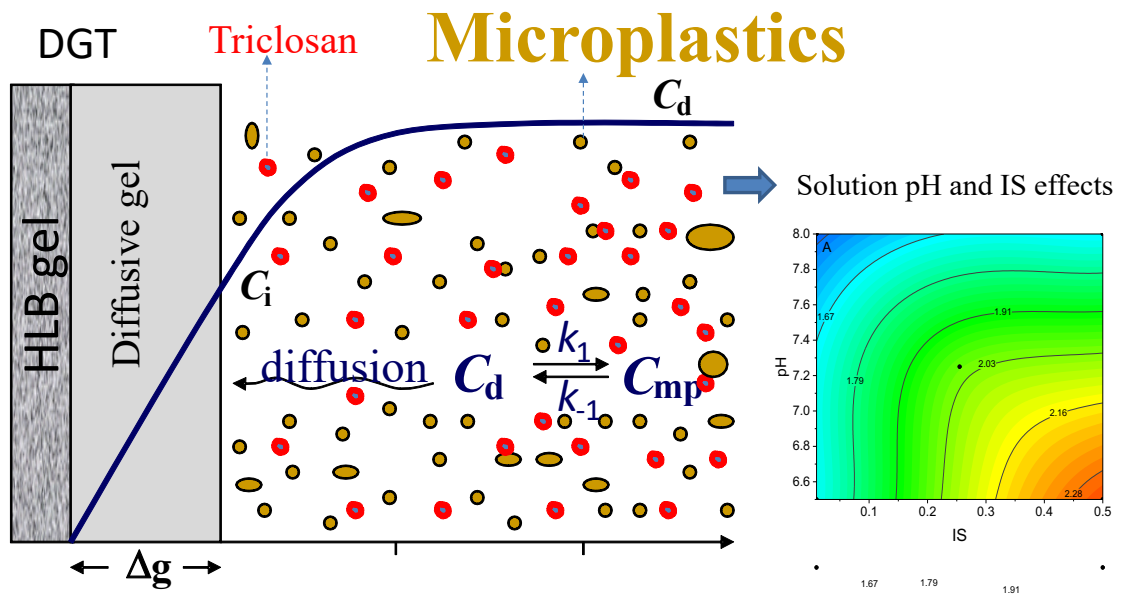
25        Microplastics (MPs) can act as vectors for chemicals, controlling the fate and  
26 potential risks posed by these chemicals. Organic chemicals associated with MPs might  
27 also pose risks as they can be released from MPs during weathering processes, although  
28 the thermodynamic and kinetics of the release processes remains poorly understood. In  
29 this study, the adsorption and desorption kinetics of triclosan (as a model compound)  
30 were investigated from two types of MPs - polystyrene (PS) and polyvinyl chloride  
31 (PVC) – by batch experiments and using the diffusive gradients in thin-films (DGT)  
32 technique as an *in-situ* tool. Batch experiments showed that pseudo-second-order  
33 equations gave the best fit for the adsorption/desorption data, implying that  
34 chemisorption is the main process. DGT continuously accumulated triclosan from MP  
35 suspensions, but slower than theoretical rates, indicating some restrictions to desorption.  
36 The DIFS model, employed to help interpret data obtained with DGT, gave distribution  
37 coefficients for labile triclosan ( $K_{dl}$ ) of 5000 mL g<sup>-1</sup> (PS) and 1000 mL g<sup>-1</sup> (PVC) and  
38 the response times ( $T_c$ ) for release of triclosan from microplastics to solution were of  
39 10 s (PS) and 1000 s (PVC). The higher  $K_{dl}$  for PS than PVC and the smaller  $T_c$  for PS  
40 than PVC show that more of the triclosan adsorbed on PS could be rapidly released,  
41 while there were some kinetic limitations for the triclosan on PVC. An important and  
42 novel finding was that key water chemistry parameters, pH and ionic strength,  
43 individually and interactively affected the supply to DGT (indicating availability). Both  
44 the  $K_{dl}$  and  $T_c$  controls the availability and hence potential risks. This is the first study  
45 to use DGT as an *in-situ* tool to quantitatively assess the interactions of organic  
46 compounds with MPs in aquatic environment, can better our understudying of fate and  
47 behaviours of MPs in environment.

48

49 **Keywords:** Microplastics; Triclosan; Diffusive Gradients in Thin-Films; sorption;  
50 waters

51

52 **Graphical Abstract**



53  
54

## 55 1. INTRODUCTION

56 Microplastics (MPs) are defined as plastic particles with a diameter less than 5 mm  
57 (Collignon et al. 2014). The most common MPs are made of Polyethylene (PE),  
58 polypropylene (PP), polystyrene (PS), polyvinyl chloride (PVC) and along with other  
59 commonly synthesised plastics, can be broken down/abraded to these small sizes in  
60 environment (MacLeod et al. 2021). MPs are now ubiquitous in oceans, rivers and even  
61 biota (Hirai et al. 2011, Law et al. 2014, Ng and Obbard 2006). MPs found in the  
62 environment may come from the additives in personal care products and polishing  
63 materials used in industrial process (primary sources) (do Sul and Costa 2014) or be  
64 formed by physical, chemical, or biological actions which break down/abrade larger  
65 pieces of plastic in the environment (secondary sources) (MacLeod et al. 2021,  
66 Rochman et al. 2013). MPs have been considered as a class of persistent pollutants  
67 which could pose negative effects on organisms, such as physical damage (Engler 2012)  
68 transformation via cytotoxicity and morphology (da Costa Araújo et al. 2020, Tu et al.  
69 2021, Wu et al. 2019), changes in lipid and energy metabolism, and alterations in gut  
70 bacterial communities (Chen et al. 2020, Wang et al. 2018). As a result, considerable  
71 attention has been paid to the environmental sources, fates and influences of MPs over  
72 the last decade or so (Galloway and Lewis 2016, Hunt et al. 2020, Lonnstedt and Eklov  
73 2016, MacLeod et al. 2021, Nizzetto et al. 2016, Stock et al. 2019).

74 MPs can adsorb chemical contaminants and carry them from one environmental  
75 compartment to another and may influence/control the fate, bioavailability and effects  
76 of contaminants that are within or on them (Liu et al. 2021, Liu et al. 2020, Sheng et al.  
77 2021, Wu et al. 2020a). Several studies have demonstrated that MPs could act as a  
78 vector of organic chemicals, such as polycyclic aromatic hydrocarbons (PAHs) and  
79 personal care product ingredients (PCPs)(Jia et al. 2020, Leon et al. 2018, Mai et al.  
80 2018, Sheng et al. 2021). Triclosan (TCS) is a typical antimicrobial agent and widely  
81 added to PCPs, such as toothpastes, cosmetics and facial cleansers (Wang et al. 2020).  
82 Raut and Angus (2010) have reported that TCS has a potential endocrine-disrupting  
83 effect on fish and it could disturb lipid and energy metabolism in tilapia fish.

84 Knowledge on the desorption process of TCS from MPs is limited to a recent study  
85 with MPs and soils (Chen et al. 2021), which reported that up to 34% and 22% of the  
86 TCS loading can be released from polyethylene (PE) and polystyrene (PS), respectively,  
87 with only one-step desorption laboratory experiments. However, it is unknown how  
88 much TCS can potentially be released if multistep desorption applies and what the  
89 desorption rates of TCS from MPs might be, which are important information that can  
90 help us to better understand the fate and ecological risks of TCS in the environment. An  
91 *in situ* technique of diffusive gradients in thin-films (DGT) (Chen et al. 2012) has been  
92 applied to compensate the disadvantages of traditional desorption batch experiments,  
93 which have been used to measure the fluxes and desorption of organic chemicals from  
94 solid phases, such as soils and sediments, with minimal disturbance (Chen et al. 2014,  
95 Chen et al. 2015, Ji et al. 2022, Li et al. 2021b). Similarly, when the DGT device is  
96 introduced into batch experiments investigating chemical-MPs desorption, it will  
97 accumulate solutes (here TCS) from the solution initially, resulting in lower interfacial  
98 concentrations which induces further TCS desorption from the MPs. How much TCS  
99 will be desorbed and how fast this process is, depends on binding strength with the MPs  
100 and also environmental conditions. Therefore, DGT can be an ideal tool to give new  
101 insights into the complex interactions between chemicals and MPs.

102 In this study, we investigate the release of TCS as an example organic contaminant  
103 from two types of MPs, PS and PVC, by using the DGT technique. The overall goal is  
104 to measure *in-situ* fluxes and release characteristics of TCS from MPs and the impacting  
105 parameters, for example pH, ionic strength (IS) and dissolved organic matter (DOM).  
106 This will enhance our understanding of the fate and behaviours of MPs associated  
107 organic chemicals, resulting in an improvement of the environmental risks.

108

## 109 **2. METHODS AND MATERIALS**

### 110 **2.1 Chemicals and Reagents**

111 Triclosan (TCS, purity > 99%) and Bisphenol A (BPA, purity > 99%) were  
112 purchased from Sigma-Aldrich and Supelco (Bellefonte, USA), respectively. BPA was

113 used as internal standard. All the standards were stored at -20 °C. PS and PVC beads  
114 (mean particle size 100 µm and 1 µm, respectively) were purchased from Hongyun  
115 Plastic Raw Materials Co., Ltd (Dongguan, China). Their infrared spectrograms and  
116 scanning electron microscopy (SEM) graphs are given in Fig. S1 of the [supporting](#)  
117 [information \(SI\)](#). Methanol and acetonitrile were all of HPLC grade and purchased from  
118 Merck (Darmstadt, Germany). Sodium chloride (NaCl), formic acid (HPLC grade) (FA),  
119 Sodium acetate (NaAc), sodium bicarbonate (NaHCO<sub>3</sub>) and hydrochloric acid (HCl) (≥  
120 25% in water) were purchased from Aladdin Reagent Inc. (Shanghai, China). DOM  
121 (humic acid) was supplied by the International Humic Substance Society. MQ water  
122 was obtained with a Purelab classic (ELGA, Antony, France).

## 123 **2.2 MP Preparation and Batch Experiments**

124 The virgin PS and PVC were washed with methanol followed by Milli-Q (MQ,  
125 18,2 ΩM) water and then oven dried before use. To prepare the PS/PVC with TCS  
126 adsorbed (contaminated PS/PVC hereafter referred to as cPS/cPVC), appropriate  
127 cleaned PS/PVC and TCS solution was equilibrated for 3 days in a 3 L conical flask  
128 with MQ water to give concentrations for PS/PVC and TCS of 1.5 g L<sup>-1</sup> and 200 ng  
129 mL<sup>-1</sup>, respectively. The MPs were then collected by a 0.7 µm GF/F filter (Whatman),  
130 dried by vacuum and stored in a glass dish at 4°C for the desorption test later.

131 To compare with the DGT method later, the adsorption and desorption kinetics of  
132 TCS on to/from the PS and PVC were tested. For the adsorption test, around 0.15 g  
133 PS/PVC were added into 100 mL of 200 ng TCS mL<sup>-1</sup> solution. The MP suspensions  
134 were continuously stirred and appropriate amounts of solution were sampled at 0, 15  
135 min, 30 min, 1h, and then 3, 5, 7, 12, 24, 36 and 48 h. The sub-samples were then  
136 filtered with a 0.22 µm polytetrafluoroethylene (PTFE) filter before analysis. By doing  
137 this, the equilibrium time was determined when the adsorption reached the maximum  
138 value and used for later experiments. In the desorption kinetics experiment, ~0.15 g  
139 cPS/cPVC were weighted in a conical flask with 50 mL MQ water. Solution samples  
140 (0.5 mL) were then collected at 0, 1, 5, 12, 24, 48 and 72 h, respectively, and filtered  
141 into GC vials before analysis.

## 142 **2.3 DGT Preparation**

143 DGT devices with 0.5 mm thick HLB-agarose binding gels and 1 mm thick  
144 agarose diffusive gels were prepared as described in a previous study (Chen et al. 2017),  
145 while no filter membrane was included to avoid significant adsorption of TCS on the  
146 filter. In brief, agarose gel solution (containing 1.5% agarose) was prepared by  
147 dissolving agarose in MQ water in a microwave oven until all the agarose was dissolved  
148 and the solution became transparent. The hot gel solution was immediately pipetted into  
149 a preheated, gel-casting assembly and left to cool down to its gelling temperature (36°C  
150 or below). For HLB-agarose binding gel, 1 g (wet weight) of HLB was added to 10 mL  
151 of hot agarose gel solution, mixed well and then cast between two preheated glass plates  
152 and left to gel at room temperature. All gels were hydrated in MQ water and stored in  
153 NaCl solution (0.01– 0.1 M).

## 154 **2.4 Desorption kinetics with DGT**

155 The MP slurries use for DGT deployment were made of 0.35 g cPS/cPVC and 15  
156 mL Milli-Q water, adding in a 60 mm diameter glass dish and mixing well. After 5 h  
157 (when TCS had reached desorption equilibrium, as determined in a preliminary test),  
158 DGT devices were deployed (exposure window facing down) in the glass dishes and  
159 left undisturbed in the bench until retrieved (duplicates DGT) after 5, 9, 24, 48, 72, 120,  
160 168, 240, 288 and 336 h, respectively. The water evaporation (though limited <5% by  
161 weight) was compensated daily with appropriate MQ water by compared to initial  
162 weight of each dish setup. The slurry temperature was measured throughout the  
163 experiment which was  $18 \pm 2$  °C.

## 164 **2.5 Effects of pH, IS, and DOM on DGT uptake**

165 To investigate the effects of pH, IS and DOM on the DGT uptake of TCS from MP  
166 slurry (with PS as an example), a three-way-two-level full factorial experimental design  
167 was employed to evaluate the main and interaction effects of these three factors. The  
168 experiment design included 8 corner points (duplicate each) and 4 central points  
169 (detailed in Table S1, SI). For each treatment, 0.35 g of cPS and 20 mL MQ water with

170 different pH, IS and DOM were added in a 60 mm diameter glass dish and mixed evenly.  
171 After 5 h, DGT devices were deployed in the glass dish for 24 h. The temperature during  
172 the experiments was recorded and was  $22.5 \pm 0.5^\circ\text{C}$ .

## 173 **2.6 Sample Preparation and Chemical analysis**

174 After deployment, three types of samples were prepared and analysed for TCS:  
175 DGT samples (providing DGT derived concentration:  $C_{\text{DGT}}$ ), the solution sample  
176 remaining at the end of the deployment (referred to as  $C_{\text{w}}$ ) and solvent extracted  
177 PS/PVC samples (referred to as  $C_{\text{mp}}$ ). For DGT samples, the extraction method for the  
178 binding gel followed our previous study (Chen et al., 2017). Briefly, the binding gels  
179 were peeled off from the DGT devices and put into a 15 mL glass vials. 5 mL of  
180 acetonitrile and the internal standard (BPA) were spiked and extracted for 30 min in an  
181 ultrasonic bath. The extract was dried with  $\text{N}_2$  gas and the sample was redissolved in 1  
182 mL mixture of acetonitrile/MQ water mixture (1:4, V:V), and filtered by 0.22  $\mu\text{m}$  PTFE  
183 syringe filter prior to be injected on to the UPLC. The solutions containing  
184 microplastics samples were collected and filtered using an empty solid phase extraction  
185 (SPE) tube with a 20  $\mu\text{m}$  sieve plate to separate from microplastics. The 0.8 mL of the  
186 collected solution was spiked with 0.2 mL acetonitrile and passed through the PTFE  
187 syringe filter (0.22  $\mu\text{m}$ ) before analysed by the UPLC; For the microplastics collected  
188 in a PP tube, methanol (5 mL) and appropriate amount of internal standard were added  
189 and extracted for 30 min in an ultrasonic bath (this provided an elution recovery of 92%  
190 as demonstrated in a preliminary test). Following this 0.5 mL of extract was taken and  
191 dried under  $\text{N}_2$  gas, and redissolved in 1 mL mixture of acetonitrile-water, and filtered  
192 by 0.22  $\mu\text{m}$  PTFE syringe filter prior to be injected on to the UPLC.

193 TCS and BPA in all samples were analysed by using an Agilent 1290 HPLC  
194 coupled with a photodiode array detector at the maximum UV absorbance of 197 and  
195 226 nm, respectively, and quantified by internal standard method. A CNW Athena C18-  
196 WP (4.6  $\times$  150 mm, 5  $\mu\text{m}$ ) LC column was used for the chemical separation. The  
197 column temperature was maintained at 30  $^\circ\text{C}$ , and the injection volume was 100  $\mu\text{L}$ .  
198 The mobile phases consisted of Mill-Q water (A) and acetonitrile (B). The gradient

199 procedure was 0–1.5 min, 50% B, then increase to 80% B within 5 min, followed by  
200 4.5 min of post-time to rebalance the column before the next injection. The  
201 quantification of TCS was performed by internal standard method with a 7 point  
202 calibration curve covering concentrations of 1 – 500 ng/mL.

203

## 204 **2.7 DGT calculation and DIFS modelling**

205 The  $C_{DGT}$  was calculated via equation (1):

$$206 \quad C_{DGT} = \frac{M \Delta g}{DA t} \quad (1)$$

207 Where:  $M$  is the mass of TCS in the DGT binding gel;  $\Delta g$  is the thickness of diffusive  
208 layer;  $D$  is the diffusion coefficient through the diffusive layer in solution, the  $D$  value  
209 for TCS was adopted from previous study (Chen et al. 2017) and calculated for  
210 temperature in this study;  $A$  is the area of DGT exposure window (3.14 cm<sup>2</sup>);  $t$  is the  
211 deployment time.

212 The DGT induced fluxes in Soils/Sediment (DIFS) model quantifies the  
213 dependence of  $R$  ( $= C_{DGT}/C_w$ ) on resupply of analyte from solid phase to solution. It  
214 uses  $K_{dl}$ , the distribution coefficient of labile analyte (eq2) and the response time,  $T_c$  (eq  
215 3), to describe the kinetics of adsorption (rate constant,  $k_1$ ) and desorption (rate constant,  
216  $k_{-1}$ ).  $K_{dl}$  may be lower than the corresponding value of  $K_d$  that is based on the total  
217 analyte measured in the solid particles.  $T_c$  is the characteristic time for the system  
218 respond to depletion by DGT.

$$219 \quad K_{dl} = \frac{C_p}{C_w} = \frac{k_1}{P_c k_{-1}} \quad (2)$$

$$220 \quad T_c = \frac{1}{k_{-1} + k_1} = \frac{1}{k_{-1}(1 + K_{dl}P_c)} \quad (3)$$

221 where  $P_c$  is the particle concentration.

222  $R$  values at different deployment time were fitted into the DIFS model to calculate  
223 the kinetic parameters ( $k_1$ ,  $k_{-1}$ , and  $T_c$ ) and  $K_{dl}$ , the input parameters are given in [Table](#)  
224 [S2](#). The software 2D\_DIFS (version 1.2.3-3, can be obtained from DGT Research Ltd,  
225 Lancaster, U.K.) was employed.

## 226 **2.8 Quality assurance and quality control**

227 An internal standard method was utilized for quantitative analysis of TCS. All data  
228 generated from the analysis were subjected to strict quality control procedures. Glass  
229 containers were chosen in the experiments, as plastic containers posed a risk of  
230 adsorption to TCS (Fig. S2). All glassware was cleaned and baked (450 °C for 4 h)  
231 before use to avoid background contamination. The method limit of detection (LOD)  
232 and limit of quantification (LOQ) for TCS were calculated using 3 and 10 times the  
233 signal-to-noise ratios and were 0.23 and 0.76 ng mL<sup>-1</sup>, respectively.

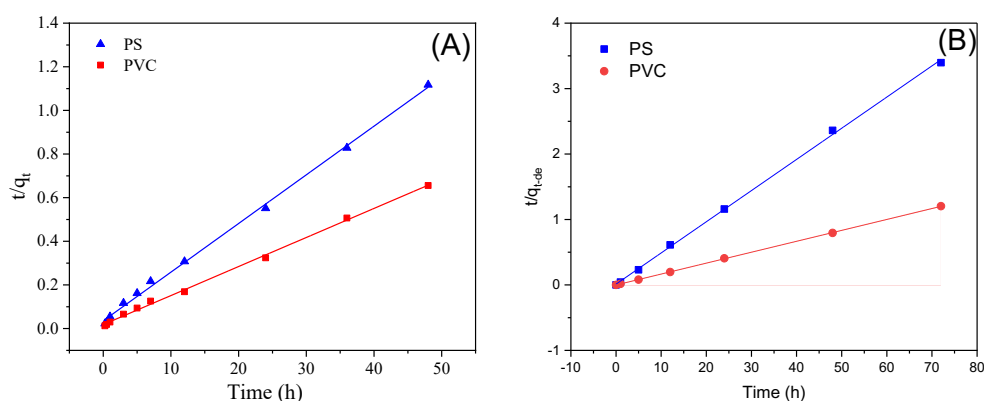
234

### 235 3. RESULTS AND DISCUSSION

#### 236 3.1 Adsorption-Desorption from the Batch Experiment

237 The results of the sorption and desorption kinetics experiments are given in Fig 1,  
238 Fig. S3 and S4 (SI). TCS was quickly adsorbed by PS and PVC and reached adsorption  
239 equilibrium after 24 h (Fig. S3A). PVC showed a higher adsorption capacity ( $q_e$ ) and  
240 uptake rate for TCS than PS (43.5 vs 74.1  $\mu\text{g g}^{-1}$ , respectively). The higher  $q_e$  for PVC  
241 could be due to its smaller particle size (therefore higher surface area) than PS,  
242 consistent with previous studies (Li et al. 2019, Velzeboer et al. 2014). Pseudo-first-  
243 order and pseudo-second-order models were used to fit the adsorption data (Fig. 1A and  
244 Fig. S3). Parameters calculated with different models for the adsorption kinetics are  
245 given in Table S3. The pseudo-second-order model gave an excellent fit for the  
246 adsorption kinetics data for both PS and PVC, with  $R^2 > 0.99$ , better than the pseudo-  
247 first-order model ( $R^2 < 0.8$ ). This finding is similar to previous studies (Chen et al. 2021,  
248 Wang and Wang 2018). The rate constants  $k_1$  and  $k_2$  were 0.118 h<sup>-1</sup> (PS), 0.085 h<sup>-1</sup> (PVC)  
249 and 0.014 g  $\mu\text{g}^{-1}\text{h}^{-1}$  (PS), 0.010 g  $\mu\text{g}^{-1}\text{h}^{-1}$  (PVC) for the first and second order models,  
250 respectively. The calculated  $q_e$  values were 44.8 and 77.2  $\mu\text{g g}^{-1}$  for PS and PVC,  
251 respectively provided by the second order model, which were comparable to the  
252 experimental  $q_e$ . The  $q_e$  of PS for TCS was much lower than those reported by previous  
253 studies (450  $\mu\text{g g}^{-1}$  (Chen et al. 2021) and 1006  $\mu\text{g g}^{-1}$  (Li et al. 2019)), probably due to  
254 the different size (Li et al. 2019, Lu et al. 2021) and crystallinity of MPs (Li et al. 2021a,  
255 Liu et al. 2019, Zhou et al. 2020). The excellent pseudo-second-order model fitting

256 suggests that the adsorption process is mainly controlled by chemical adsorption rather  
257 than physical adsorption (Lu et al. 2021).



258

259 **Fig. 1** Adsorption (A) and desorption (B) kinetics modelling (pseudo-second-order) of  
260 TCS on to/from PS and PVC in the batch experiment.

261 For the desorption stage, TCS desorbed from PS and PVC in 12 h and reached  
262 desorption equilibrium after 24 h (Fig. 1B and Fig. S4). The percentage of TCS that  
263 desorbed from PS (32.9%) was over twice that from PVC (13.3%), indicating the strong  
264 interaction of TCS with PVC and that the adsorbed TCS on the MPs are partially labile  
265 (implying availability). The pseudo-second-order model also fitted the desorption data  
266 very well ( $R^2 > 0.99$ ) for both PS and PVC (Table S4), an improvement compared to  
267 the pseudo-first-order model ( $R^2 < 0.4$ ), again suggesting that the desorption process of  
268 TCS from MPs is mainly controlled by chemical adsorption (Lu et al. 2021). The  
269 desorption rate constants ( $k_2$ ) followed the order of PS ( $0.181 \text{ g } \mu\text{g}^{-1}\text{h}^{-1}$ ) > PVC ( $-0.484$   
270  $\text{g } \mu\text{g}^{-1}\text{h}^{-1}$ ), which also exhibited the strong binding of TCS to PVC (Table S3). The  
271 calculated sorption capacities in the desorption phase ( $q_{e,de}$ ) were  $21.0 \text{ } \mu\text{g g}^{-1}$  and  $59.9$   
272  $\text{ } \mu\text{g g}^{-1}$  for PS and PVC, respectively, very close to the experimental values ( $20.5 \text{ } \mu\text{g g}^{-1}$   
273 for PS and  $60.0 \text{ } \mu\text{g g}^{-1}$  for PVC).

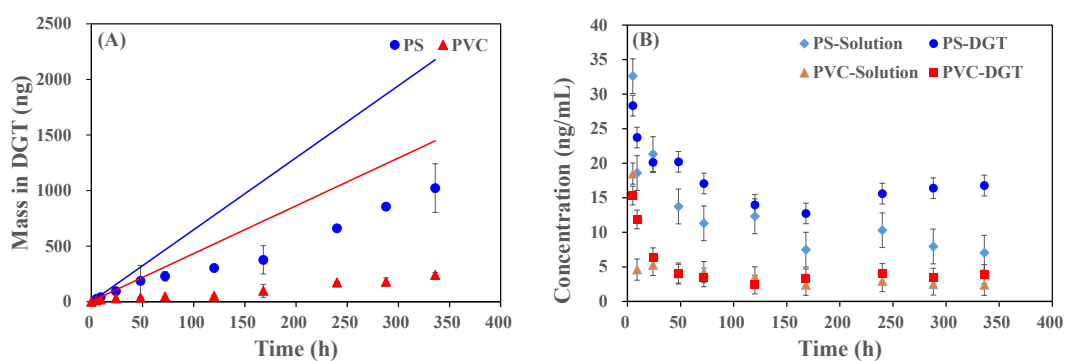
274

### 275 3.2 Desorption driven by DGT and DIFS modelling

276 When DGT is deployed within the suspensions containing MPs, it will firstly take  
277 up the TCS from the dissolved phase, which then induces desorption of TCS previously

278 adsorbed on the MPs. This broadly mimics uptake processes for biota. Therefore,  
 279 understanding these processes helps enhance our knowledge of the potential  
 280 bioavailability of chemicals adsorbed on MPs. The measured masses of TCS  
 281 accumulated by DGT after different deployment times are shown in Fig. 2A. As can be  
 282 seen, DGT accumulated much more TCS from PS than PVC, consistent with the results  
 283 from the batch experiment. However, DGT accumulated masses of TCS that were much  
 284 lower than the theoretical values (assuming unchanging solution concentrations) for  
 285 both PS and PVC. This indicates that the desorption of TCS from MPs induced by DGT  
 286 is limited by the rate of supply/ desorption rate (kinetically) from the MPs. The DGT  
 287 derived concentrations ( $C_{DGT}$ ) and the directly measured solution concentrations ( $C_w$ )  
 288 of TCS are compared in Fig. 2B. Both decreased with increasing deployment time from  
 289 both the PS and PVC, but the reduction was more pronounced for PVC. TCS on PS is  
 290 more readily available and supplied to solution more quickly.

291



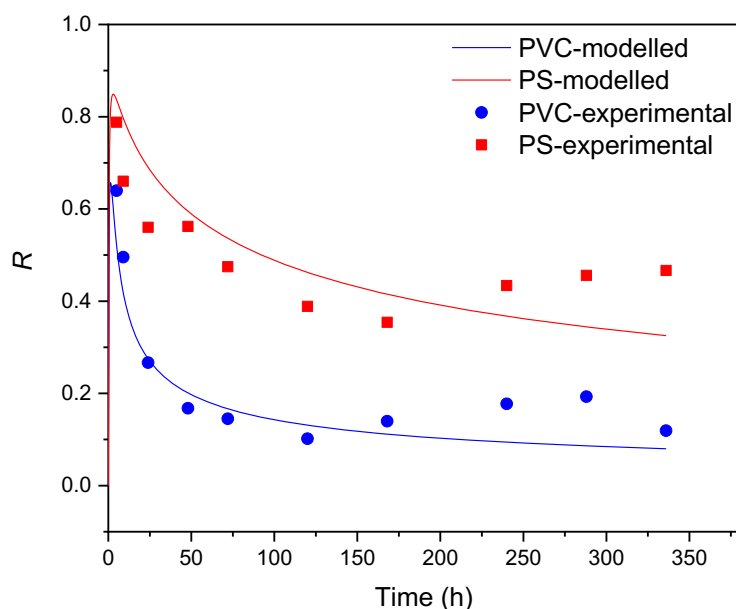
292

293 **Fig. 2** Dependence on deployment times of the DGT accumulated masses of TCS from  
 294 PS or PVC for different DGT deployment times (A) and the DGT derived TCS  
 295 concentrations and direct solution measurements (B). The blue and red lines represent  
 296 theoretical accumulated masses by DGT for PS and PVC, respectively. They were  
 297 calculated according to the equation  $M = \frac{DC_{w0}At}{\Delta g + \delta}$ , re-arranged from equation (1), where  
 298  $C_{w0}$  is the initial concentration of TCS in the solution,  $\delta$  is the thickness of diffusive  
 299 boundary layer with value of 0.76 mm adopted from our previous study at static  
 300 condition (Chen et al. 2012).

301

302 To obtain quantitative desorption kinetic data, the experimental data ( $R$  at different  
303 times) were applied to the DIFS model. Because the experimental setup was limited to  
304 20 mL, rather than an infinite system/volume, to calculate the ratio of  $R$  that is required  
305 for the DIFS model, the initial solution concentration of TCS ( $C_{w0}$ ) was used. Other  
306 parameters for the DIFS model are given in Table S2. The observed  $R$  and modelled  $R$   
307 from the best fit were plotted against deployment time for TCS in solutions with PS or  
308 PVC and are given in Fig. 3.

309 The DIFS model fitted the experimental data well, particularly over short time  
310 periods, with a general trend of an initial decline in  $R$ , followed by a slower decrease  
311 particularly over longer time periods. This is very similar to a previous study for  
312 antibiotics in soils (Chen et al. 2014). In theory, and as observed in the modelled line,  
313 there should be an initial increase for  $R$  due to the establishment of a linear diffusion  
314 gradient in the diffusive layer. There was no TCS in solution at the beginning, quickly  
315 reaching a maximum. However, this was too fast to be observed before the first data  
316 point at 5 h. The later decline in  $R$  reflects the decreased concentration of TCS at the  
317 DGT interface and therefore the solution in this relatively small system. The decrease  
318 in the solution TCS concentration caused disequilibrium between the solution and MP  
319 phases, inducing desorption from the MP to resupply the solution phase. However, this  
320 desorption was not fast enough to fully resupply the decrease in the solution phase, so  
321  $R$  continuously decreased. The greater decline in  $R$  for PVC than PS indicates that the  
322 ability of PVC to resupply TCS is less than that of PS. Larger  $R$  values for PS than PVC  
323 at the same time points suggests a faster resupply (shorter response time) of TCS on PS  
324 as documented as follow.



325

326 **Fig. 3** DIFS modelling of  $R$  ( $C_{DGT}/C_{w0}$ ) against time for TCS in the suspensions with  
 327 PS and PVC.

328

329 **Table 1.** Parameters for TCS desorption from PS and PVC derived from the best DIFS  
 330 model fitting

Parameter	PS	PVC
$K_d$ (mL g <sup>-1</sup> )*	1874	7483
$K_{dl}$ (mL g <sup>-1</sup> )	4667	906
$T_c$ (s)	10	1005
$k_1$ (s <sup>-1</sup> )	$9.8 \times 10^{-2}$	$9.5 \times 10^{-4}$
$k_{-1}$ (s <sup>-1</sup> )	$1.2 \times 10^{-3}$	$4.5 \times 10^{-5}$

331

\*obtained from the methanol extraction method.

332

333

334

335

336

337

338

339

The resulting thermodynamic ( $K_{dl}$ ) and kinetic parameters ( $T_c$ ,  $k_1$  and  $k_{-1}$ ) from the best DIFS model fitting are given in [Table 1](#), together with the experimental  $K_d$  for comparison. For PS, the  $K_{dl}$  value is greater than the  $K_d$ , which indicates that the labile TCS is adsorbed on the PS is much larger than that estimated by the methanol extraction, suggesting that simple solvent extraction might underestimate the availability of TCS on PS. In contrast, for PVC, the  $K_{dl}$  is much smaller than the  $K_d$ , indicating that the labile fraction on the PVC is much smaller than the methanol extracted fraction (which overestimates the availability). This implies that the TCS bound onto the PVC is less

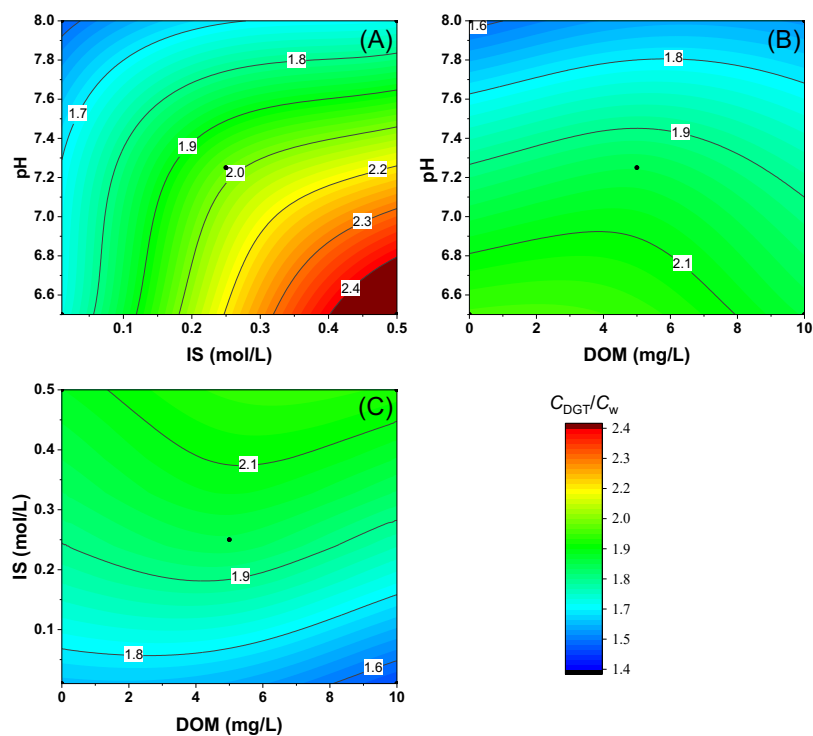
340 available than that on the PS; there is a much smaller labile pool of TCS on PVC though  
341 with a much higher  $K_d$ .

342  $K_{dl}$  ultimately controls the amount of TCS that could be desorbed from MPs, while  
343  $T_c$  and  $k_{-1}$  determine how fast MPs can release TCS to the solution (Chen et al. 2014,  
344 Harper et al. 1998).  $T_c$  values for PVC were 2 orders of magnitudes higher than for PS,  
345 indicating that the TCS is released more rapidly to the solution from PS, and it takes  
346 longer for PVC (~17 min) compared to PS (< half minute) to reflect the decline of TCS  
347 in solution. The resulting  $k_1$  values for PS are much higher than the corresponding  
348 adsorption rate constants ( $0.018 \text{ h}^{-1} - 26 \text{ h}^{-1}$ ) from the batch experiment method (with  
349 pseudo-first-order model) reported in previous studies (Chen et al. 2021, Lu et al. 2021,  
350 Wu et al. 2020b). For PVC, they are similar to or slightly higher than the corresponding  
351 values ( $0.037 \text{ h}^{-1} - 1.4 \text{ h}^{-1}$ ) obtained previously (Lu et al. 2021, Ma et al. 2019). This is  
352 likely because the pseudo-first-order model cannot describe the process well in many  
353 cases as documented in these studies. Relatively few  $k_{-1}$  values ( $0.032 \text{ h}^{-1} - 0.080 \text{ h}^{-1}$ )  
354 (Chen et al. 2021, Lu et al. 2021) are available for MPs, and they are close to our values  
355 from the batch experiment but again less than those from the DGT and DIFS simulated  
356 values. Smaller  $k_{-1}$  for PVC than PS implies there is a greater kinetic limitation for the  
357 release of TCS from PVC, but not for PS.

358

### 359 **3.3 Effects of IS, pH and DOM**

360 In actual aquatic environments, some key water chemistry parameters such as pH,  
361 IS, DOM can affect/control the fate, behaviour and availability of analytes of interest.  
362 DGT can mimic, to some extent, biota that uptake chemicals from solution in the  
363 presence of solids such as in soil/sediment. DGT was used in this work to provide an  
364 estimation/comparison of the labile fraction of TCS released from MPs (with PS as an  
365 example) under different conditions with varying of these water chemistry parameters.  
366 The results for the effects of these binary parameters on DGT measurements (expressed  
367 as  $r$  – indicator of capability for release of TCS from solid phase to solution) are shown  
368 in Fig. 4.



369

370 **Fig.4** Interaction effects of (A) pH and ionic strength (IS), (B) dissolved organic matter  
 371 (DOM) and pH, and (C) DOM and IS on the ratio ( $r$ ) of DGT derived concentration  
 372 ( $C_{DGT}$ ) and directly measured solution concentration ( $C_w$ ) of TCS from solutions  
 373 containing PS MPs within 24 hours.

374 The statistical analysis (Table S5 and Fig. S5) shows that the solution IS, pH and  
 375 their interaction (IS\*pH) had significant effects on the value of  $r$  ( $p < 0.05$ ), while no  
 376 significant effect was observed for DOM or its interaction with IS or pH ( $p > 0.05$ ). As  
 377 shown in Fig. 4, the value of  $r$  decreased as pH increased, and increased as IS increased.  
 378 Lower pH resulted in less TCS being released from PS. Previous studies have also  
 379 reported adsorption decreasing with increasing pH; this is due to the chemical  
 380 speciation changes (resulting in electrostatic repulsion for the increasing negative  
 381 charged target chemicals) (Li et al. 2019, Sun et al. 2021, Wu et al. 2020b). Higher IS  
 382 suppressed the release of analyte from MPs to solution, which has also been reported in  
 383 other studies (Lu et al. 2021, Wu et al. 2020b). However, for the first time, we  
 384 investigated the interaction effect of these parameters in this study, and found that the  
 385 effects of pH and IS are dependent on each other (Fig 4A). For example, at lower IS  
 386 (such as  $< 0.05$  mol/L), the effect of pH might be not significant, while at higher IS, pH

387 showed significant effects; Similarly, the IS effect might be negligible at high pH (e.g. >  
388 7.8) but significant when the pH is lower. Clearly, conditions with higher IS and lower  
389 pH will result in more TCS being available while lower IS and higher pH will make  
390 TCS on MPs less available; conditions with lower IS and pH or higher IS and pH will  
391 result in similar (medium) TCS availability in the solutions. This implies that the  
392 availability and risks of chemicals on MPs change as environmental conditions change.  
393 For example, from freshwater (low IS) to seawater (high pH and high IS), the  
394 availability of contaminants on MPs might firstly increase then decrease, which might  
395 result in no apparent changes. While in some scenarios, such as in stomach of animals  
396 (carrying MPs with micropollutants (Liu et al. 2020)), where the pH is lower and if the  
397 IS is higher at the same time, more chemicals will be released and available for uptake  
398 resulting in higher risks for the animals. No measurable effects of DOM on the value  
399 of  $r$  was observed probably because all the freely dissolved and DOM associated TCS  
400 were available for DGT uptake under these test conditions. Therefore, interaction  
401 effects from these parameters, particularly pH and IS, should be considered in toxicity  
402 studies and risk assessments for MPs with adsorbed micropollutants.

403

#### 404 **4. Conclusions and Perspectives**

405 This study has, for the first time, assessed the desorption and release of TCS as a  
406 model compound from MPs, using the DGT technique. Compared to the batch  
407 experiment approach, the DGT method provides both thermodynamic and kinetic  
408 information, whilst potentially also mimicking chemical availability to biota from the  
409 MPs, although more dedicated studies are warranted. DGT can act as an almost infinite  
410 sink for the analytes of interest and provides an assessment of the availability of  
411 analytes desorbed from MPs. Results from this study suggest that the labile fraction of  
412 TCS is controlled by MP type. The water chemistry parameters pH and IS are key  
413 factors affecting the availability of analytes on MPs, but are not independent of each  
414 other. As a result, they should be taken into consideration at the same time, particularly  
415 for environments characterized by varying pH and IS in space, such as river/estuaries

416 and the intestinal tracts of organisms (Liu et al. 2020). The uptake by DGT of inorganic  
417 substances in aquatic systems has been demonstrated to correlate well with their  
418 concentration/toxicity in biota (Costello et al. 2012, Xie et al. 2021). Hence, findings  
419 from this work might also apply to the uptake processes of organic chemicals by biota.  
420 Our findings might all also help the study design and/or data interpretation for  
421 microplastics with co-existing contaminants. Our work here demonstrated that DGT  
422 can be a promising in situ tool for understanding the fate, behaviour and effects of  
423 organic contaminants (theoretically also for inorganics) adsorbed on microplastics. This  
424 should provide data to improve the risk assessment of emerging contaminants and  
425 microplastics.

426

## 427 **Acknowledgements**

428 This work was financially supported by the Key Deployment Project of Centre for  
429 Ocean Mega-Research of Science, Chinese Academy of Sciences (COMS2019J08),  
430 Guangzhou Municipal Science and Technology Project (No. 201904010291), National  
431 Natural Science Foundation of China (No. 21806042) and Guangdong Provincial Key  
432 Laboratory of Chemical Pollution and Environmental Safety (2019B030301008). The  
433 authors are grateful to Prof. Hao Zhang and Prof. Kevin C. Jones for their kind  
434 comments/suggestion on the drafted manuscript. Miss Y. W. Jia is supported by Chinese  
435 Scholarship Council (PhD fellowship 202006750030).

## 436 **Notes**

437 The authors declare no competing financial interest.

## 438 **References**

- 439 Chen, C.-E., Jones, K.C., Ying, G.-G. and Zhang, H. (2014) Desorption Kinetics of Sulfonamide and  
440 Trimethoprim Antibiotics in Soils Assessed with Diffusive Gradients in Thin-Films. *Environmental*  
441 *Science & Technology* 48(10), 5530-5536.
- 442 Chen, C.E., Chen, W., Ying, G.G., Jones, K.C. and Zhang, H. (2015) In situ measurement of solution  
443 concentrations and fluxes of sulfonamides and trimethoprim antibiotics in soils using o-DGT.  
444 *Talanta* 132, 902-908.
- 445 Chen, C.E., Zhang, H. and Jones, K.C. (2012) A novel passive water sampler for in situ sampling of  
446 antibiotics. *Journal of Environmental Monitoring* 14(6), 1523-1530.

447 Chen, Q.Q., Li, Y. and Li, B.W. (2020) Is color a matter of concern during microplastic exposure to  
448 *Scenedesmus obliquus* and *Daphnia magna*? *Journal of Hazardous Materials* 383.

449 Chen, W., Li, Y.Y., Chen, C.E., Sweetman, A.J., Zhang, H. and Jones, K.C. (2017) DGT Passive  
450 Sampling for Quantitative in Situ Measurements of Compounds from Household and Personal  
451 Care Products in Waters. *Environmental Science & Technology* 51(22), 13274-13281.

452 Chen, X., Gu, X., Bao, L., Ma, S. and Mu, Y. (2021) Comparison of adsorption and desorption of  
453 triclosan between microplastics and soil particles. *Chemosphere* 263, 127947.

454 Collignon, A., Hecq, J.H., Galgani, F., Collard, F. and Goffart, A. (2014) Annual variation in neustonic  
455 micro- and meso-plastic particles and zooplankton in the Bay of Calvi (Mediterranean-Corsica).  
456 *Marine Pollution Bulletin* 79(1-2), 293-298.

457 Costello, D.M., Burton, G.A., Hammerschmidt, C.R. and Taulbee, W.K. (2012) Evaluating the  
458 Performance of Diffusive Gradients in Thin Films for Predicting Ni Sediment Toxicity. *Environmental  
459 Science & Technology* 46(18), 10239-10246.

460 da Costa Araújo, A.P., de Melo, N.F.S., de Oliveira Junior, A.G., Rodrigues, F.P., Fernandes, T., de  
461 Andrade Vieira, J.E., Rocha, T.L. and Malafaia, G. (2020) How much are microplastics harmful to the  
462 health of amphibians? A study with pristine polyethylene microplastics and *Physalaemus cuvieri*.  
463 *Journal of Hazardous Materials* 382, 121066.

464 do Sul, J.A.I. and Costa, M.F. (2014) The present and future of microplastic pollution in the marine  
465 environment. *Environmental Pollution* 185, 352-364.

466 Engler, R.E. (2012) The Complex Interaction between Marine Debris and Toxic Chemicals in the  
467 Ocean. *Environmental Science & Technology* 46(22), 12302-12315.

468 Galloway, T.S. and Lewis, C.N. (2016) Marine microplastics spell big problems for future  
469 generations. *Proceedings of the National Academy of Sciences of the United States of America*  
470 113(9), 2331-2333.

471 Harper, M.P., Davison, W., Zhang, H. and Tych, W. (1998) Kinetics of metal exchange between  
472 solids and solutions in sediments and soils interpreted from DGT measured fluxes. *Geochimica et  
473 Cosmochimica Acta* 62(16), 2757-2770.

474 Hirai, H., Takada, H., Ogata, Y., Yamashita, R., Mizukawa, K., Saha, M., Kwan, C., Moore, C., Gray, H.,  
475 Laursen, D., Zettler, E.R., Farrington, J.W., Reddy, C.M., Peacock, E.E. and Ward, M.W. (2011)  
476 Organic micropollutants in marine plastics debris from the open ocean and remote and urban  
477 beaches. *Marine Pollution Bulletin* 62(8), 1683-1692.

478 Hunt, C.F., Lin, W.H. and Voulvoulis, N. (2020) Evaluating alternatives to plastic microbeads in  
479 cosmetics. *Nature Sustainability* 4(4), 366-372.

480 Ji, X., Challis, J.K., Cantin, J., Cardenas Perez, A.S., Gong, Y., Giesy, J.P. and Brinkmann, M. (2022) A  
481 novel passive sampling and sequential extraction approach to investigate desorption kinetics of  
482 emerging organic contaminants at the sediment–water interface. *Water Research* 217, 118455.

483 Jia, Y.-W., Huang, Z., Hu, L.-X., Liu, S., Li, H.-X., Li, J.-L., Chen, C.-E., Xu, X.-R., Zhao, J.-L. and Ying,  
484 G.-G. (2020) Occurrence and mass loads of biocides in plastic debris from the Pearl River system,  
485 South China. *Chemosphere* 246, 125771.

486 Law, K.L., Moret-Ferguson, S.E., Goodwin, D.S., Zettler, E.R., De Force, E., Kukulka, T. and  
487 Proskurowski, G. (2014) Distribution of Surface Plastic Debris in the Eastern Pacific Ocean from an  
488 11-Year Data Set. *Environmental Science & Technology* 48(9), 4732-4738.

489 Leon, V.M., Garcia, I., Gonzalez, E., Samper, R., Fernandez-Gonzalez, V. and Muniategui-Lorenzo,

490 S. (2018) Potential transfer of organic pollutants from littoral plastics debris to the marine  
491 environment. *Environmental Pollution* 236, 442-453.

492 Li, H., Wang, F., Li, J., Deng, S. and Zhang, S. (2021a) Adsorption of three pesticides on polyethylene  
493 microplastics in aqueous solutions: Kinetics, isotherms, thermodynamics, and molecular dynamics  
494 simulation. *Chemosphere* 264, 128556.

495 Li, Y., Han, C., Luo, J., Jones, K.C. and Zhang, H. (2021b) Use of the Dynamic Technique DGT to  
496 Determine the Labile Pool Size and Kinetic Resupply of Pesticides in Soils and Sediments.  
497 *Environmental Science & Technology* 55(14), 9591-9600.

498 Li, Y.D., Li, M., Li, Z., Yang, L. and Liu, X. (2019) Effects of particle size and solution chemistry on  
499 Triclosan sorption on polystyrene microplastic. *Chemosphere* 231, 308-314.

500 Liu, F.F., Liu, G.Z., Zhu, Z.L., Wang, S.C. and Zhao, F.F. (2019) Interactions between microplastics  
501 and phthalate esters as affected by microplastics characteristics and solution chemistry.  
502 *Chemosphere* 214, 688-694.

503 Liu, G., Dave, P.H., Kwong, R.W.M., Wu, M. and Zhong, H. (2021) Influence of Microplastics on the  
504 Mobility, Bioavailability, and Toxicity of Heavy Metals: A Review. *Bulletin of Environmental  
505 Contamination and Toxicology* 107(4), 710-721.

506 Liu, X.L., Gharasoo, M., Shi, Y., Sigmund, G., Huffer, T., Duan, L., Wang, Y.F., Ji, R., Hofmann, T. and  
507 Chen, W. (2020) Key Physicochemical Properties Dictating Gastrointestinal Bioaccessibility of  
508 Microplastics-Associated Organic Xenobiotics: Insights from a Deep Learning Approach.  
509 *Environmental Science & Technology* 54(19), 12051-12062.

510 Lonnstedt, O.M. and Eklov, P. (2016) Environmentally relevant concentrations of microplastic  
511 particles influence larval fish ecology (Retracted Article). *Science* 352(6290), 1213-1216.

512 Lu, J., Wu, J., Wu, J., Zhang, C. and Luo, Y. (2021) Adsorption and Desorption of Steroid Hormones  
513 by Microplastics in Seawater. *Bulletin of Environmental Contamination and Toxicology* 107(4), 730-  
514 735.

515 Ma, J., Zhao, J., Zhu, Z., Li, L. and Yu, F. (2019) Effect of microplastic size on the adsorption behavior  
516 and mechanism of triclosan on polyvinyl chloride. *Environmental Pollution* 254(Pt B), 113104.

517 MacLeod, M., Arp, H.P.H., Tekman, M.B. and Jahnke, A. (2021) The global threat from plastic  
518 pollution. *Science* 373(6550), 61-65.

519 Mai, L., Bao, L.J., Shi, L., Liu, L.Y. and Zeng, E.Y. (2018) Polycyclic aromatic hydrocarbons affiliated  
520 with microplastics in surface waters of Bohai and Huanghai Seas, China. *Environmental Pollution*  
521 241, 834-840.

522 Ng, K.L. and Obbard, J.P. (2006) Prevalence of microplastics in Singapore's coastal marine  
523 environment. *Marine Pollution Bulletin* 52(7), 761-767.

524 Nizzetto, L., Langaas, S. and Futter, M. (2016) Do microplastics spill on to farm soils? *Nature*  
525 537(7621), 488-488.

526 Rochman, C.M., Hoh, E., Kurobe, T. and Teh, S.J. (2013) Ingested plastic transfers hazardous  
527 chemicals to fish and induces hepatic stress. *Scientific Reports* 3, 3263.

528 Sheng, C., Zhang, S.H. and Zhang, Y. (2021) The influence of different polymer types of  
529 microplastics on adsorption, accumulation, and toxicity of triclosan in zebrafish. *Journal of  
530 Hazardous Materials* 402, 123733.

531 Stock, F., Kochleus, C., Bänsch-Baltruschat, B., Brennholt, N. and Reifferscheid, G. (2019) Sampling  
532 techniques and preparation methods for microplastic analyses in the aquatic environment – A  
533 review. *TrAC Trends in Analytical Chemistry* 113, 84-92.

534 Sun, P., Liu, X., Zhang, M., Li, Z., Cao, C., Shi, H., Yang, Y. and Zhao, Y. (2021) Sorption and leaching  
535 behaviors between aged MPs and BPA in water: The role of BPA binding modes within plastic  
536 matrix. *Water Research* 195, 116956.

537 Tu, C., Liu, Y., Li, L., Li, Y., Vogts, A., Luo, Y. and Waniek, J.J. (2021) Structural and Functional  
538 Characteristics of Microplastic Associated Biofilms in Response to Temporal Dynamics and Polymer  
539 Types. *Bulletin of Environmental Contamination and Toxicology* 107(4), 633-639.

540 Velzeboer, I., Kwadijk, C.J.A.F. and Koelmans, A.A. (2014) Strong Sorption of PCBs to Nanoplastics,  
541 Microplastics, Carbon Nanotubes, and Fullerenes. *Environmental Science & Technology* 48(9),  
542 4869-4876.

543 Wang, F., Wong, C.S., Chen, D., Lu, X.W., Wang, F. and Zeng, E.Y. (2018) Interaction of toxic  
544 chemicals with microplastics: A critical review. *Water Research* 139, 208-219.

545 Wang, W.F. and Wang, J. (2018) Comparative evaluation of sorption kinetics and isotherms of  
546 pyrene onto microplastics. *Chemosphere* 193, 567-573.

547 Wu, B., Wu, X.M., Liu, S., Wang, Z.Z. and Chen, L. (2019) Size-dependent effects of polystyrene  
548 microplastics on cytotoxicity and efflux pump inhibition in human Caco-2 cells. *Chemosphere* 221,  
549 333-341.

550 Wu, P., Tang, Y., Jin, H., Song, Y., Liu, Y. and Cai, Z. (2020a) Consequential fate of bisphenol-  
551 attached PVC microplastics in water and simulated intestinal fluids. *Environmental Science and*  
552 *Ecotechnology* 2, 100027.

553 Wu, X., Liu, P., Huang, H. and Gao, S. (2020b) Adsorption of triclosan onto different aged  
554 polypropylene microplastics: Critical effect of cations. *Science of the Total Environment* 717,  
555 137033.

556 Xie, M., Simpson, S.L., Huang, J., Teasdale, P.R. and Wang, W.-X. (2021) In Situ DGT Sensing of  
557 Bioavailable Metal Fluxes to Improve Toxicity Predictions for Sediments. *Environmental Science &*  
558 *Technology* 55(11), 7355-7364.

559 Zhou, Y.F., Yang, Y.Y., Liu, G.H., He, G. and Liu, W.Z. (2020) Adsorption mechanism of cadmium on  
560 microplastics and their desorption behavior in sediment and gut environments: The roles of water  
561 pH, lead ions, natural organic matter and phenanthrene. *Water Research* 184, 116209.

562